Catalysis Today 147S (2009) S295–S300

Contents lists available at ScienceDirect

Catalysis Today

journal homepage: www.elsevier.com/locate/cattod

Experimental investigation of soot deposition in diesel particulate filters

S. Bensaid, D.L. Marchisio, N. Russo, D. Fino *

Dipartimento di Scienza dei Materiali ed Ingegneria Chimica, Politecnico di Torino, Corso Duca degli Abruzzi 24, 10129, Torino, Italy

ARTICLE INFO

Article history:
Available online 3 August 2009

Keywords:
Diesel particulate filter
Soot filtration
Multiphase flow
Particle deposition
Porous media
Computational fluid dynamics

ABSTRACT

The present paper highlights the features of soot deposition inside the channels of wall-flow diesel particulate filters (DPFs). This investigation is tailored to understand the behaviour of soot loading in DPFs, since the subsequent regeneration step is strongly affected by the cake profile in the inner channels of the filter. In addition, the experimental data here reported are useful to validate detailed mathematical models for the prediction of pressure drop, filtration efficiency and filter loading.

The investigation regards the differences in soot deposition profiles of two geometries for the filter housing: the first one was responsible for an uneven distribution of the flow at the inlet of the channel, closer to real cases in the exhaust pipes, while the other one was designed to minimize this effect. The two housings were tested in the same operating conditions, with lab-scale filters and synthetic soot, in order to achieve a better reproducibility of the inlet conditions, rather than with real diesel soot from a diesel engine. The evolution of soot deposition profiles at different loading times was monitored as well. Furthermore, the filtration efficiency was evaluated through measurements of particle size distributions before and after the filter.

Some conclusions regarding the most appropriate mathematical model to simulate these phenomena are reported at the end of the paper, with reference to our past modelling activity.

1. Introduction

There is an established awareness concerning the health effects caused by soot emissions of diesel exhausts in automotive applications [1]. It is widely accepted that soot particles emitted by diesel engines act as carriers for a number of harmful substances and long-term exposure to fine particulate matter is a proven risk factor for respiratory and cardiovascular diseases, as suggested by many authors [2,3].

Nowadays, soot emissions can be reduced by physically trapping the particles with on-board wall-flow diesel particulate filters (DPFs). Particulate is collected onto the surface of the inlet channels, thus causing an increasing pressure drop, until regeneration is carried out to ignite the filtered soot. Filtration in DPFs is characterized by two subsequent phases:

(1) Soot particles (normally laying in the sub micron range) are at first trapped in the filter pores, mainly under the action of Brownian motions and interception mechanisms [4], resulting in a gradual reduction of porosity and permeability [5]; this phase is known as depth filtration.

(2) The regions of the filter where the maximum packing density is reached become "impermeable" to the particles, and a soot layer onto the porous filter surface is built up. During this phase, called cake formation, an additional pressure drop is generated, which increases linearly with time, along with the soot layer growth [5].

After the pressure drop has reached a maximum allowable value, entailing a too high fuel penalty, regeneration of the filter is induced by post-injecting some fuel, which burns in an upstream catalytic converter and heats up the exhaust gases until the soot ignition temperature is reached. This operation can be either catalytic or not: in the former case a catalyst is deposited onto the surface of the channel walls to promote soot combustion at lower temperatures compared to standard traps [6], thus resulting in remarkable fuel savings. Experimental evidences clearly show that crucial parameters during regeneration are the gas inlet temperature, the residual oxygen concentration and the local filter soot loading (especially in terms of deposition profiles across the filter channels) [7,8]. It is therefore clear that a detailed investigation of the filtration process is necessary to efficiently carry out the DPF regeneration.

To this end, spatial distributions of soot particles inside the DPF channels, at the end of a loading cycle, are experimentally investigated in the present work. Some authors have attempted

* Corresponding author. Tel.: +39 011 0904710; fax: +39 011 0904699.
E-mail address: debora.fino@polito.it (D. Fino).

0920-5861/$ – see front matter © 2009 Elsevier B.V. All rights reserved.
doi:10.1016/j.cattod.2009.07.039

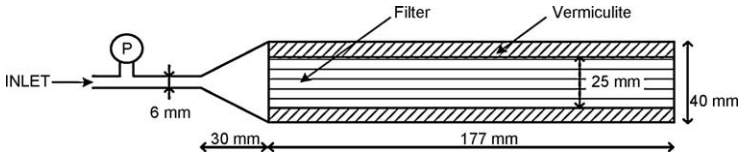

Fig. 1. Sketch of the first filter housing.

to investigate the characteristics of soot loading, mainly with the purpose of validating simulation tools for the prediction of the DPF pressure drop [9,10]. They focused on soot deposition on single channels physically extracted from full-scale DPFs, and loaded either in parallel with a full-scale DPF to ensure realistic pressure drop conditions [10], or through the tailored control of the flow into the channel [9]. On the contrary, in this work the experimental investigation involved the whole DPF, thus collecting for the first time information concerning soot deposition inside the filter under real loading conditions. Hence, the internal flow field in the channels is responsible for soot deposition profiles, and with our experimental procedure no modifications to it were introduced. After the DPF loading, the lab-scale filter was sectioned and the soot layer thickness was measured in each channel, as later described. Since the soot loading inside the different channels depends on the gas velocity profile at the filter inlet, the effect of the filter housing geometry was investigated. To this end, two different housing geometries were analysed: the first one was responsible for a strong maldistribution of the gas velocity profile at the filter inflow, while with the other one a rather uniform distribution occurred. The experimental characterisation of the cake profiles was carried out at two different loading times, in order to track the thickening evolution of the soot layer.

A parameter of major importance in DPFs is the filtration efficiency, expressed by the probability of successful collection of soot particles in the pores of the filter and, during cake filtration, on the soot layer itself. The filtration efficiency of the DPF was therefore investigated through measurements of the particle size distribution at the inlet and the outlet of the filter. The filtration efficiency at the beginning of the filtration process defines the ability of the bare filter to collect particles, and it is normally quite low. As soot is collected, it becomes the real filtering media and the efficiency increases considerably [11]. All these features were experimentally observed.

The influence of the gas inlet flow on the DPF behaviour has been widely investigated in the literature [12,13], also regarding the dynamics of soot regeneration, and the consequent transient modification of the permeability in the full-scale filter channels due to different soot oxidation rates. The experimental data we collected were employed to show some conclusions about the most suitable computational fluid dynamics model, also resorting to our present and past modelling activity [14,15].

2. Experimental and numerical details

The experimental rig consisted of a testing apparatus for lab-scale DPFs (17.7 cm long and 2.54 cm in diameter), having 300 cpsi and an average porosity of 43%. As mentioned, two different filter housings were investigated. Fig. 1 reports the sketch of the first test rig, characterized by a 4 cm pipe diameter (where the filter was located), connected through a conic surface to the gas inlet pipe (6 mm in diameter). The pressure sampling point was located before the conic junction, while the end of the filter was at ambient pressure. As a result, the total measured pressure drop included the expansion losses in the conic junction.

The second test rig is depicted in Fig. 2: the filter was canistered in a 3.8 cm pipe diameter, having a much longer inflow region (150 mm), a less pronounced conic junction (90 mm instead of 30 mm in Fig. 1), and a greater inlet pipe diameter (10 mm instead of 6 mm) affecting the gas velocity. In this housing geometry, the pressure was measured at the front and at the back of the filter (sampling points are denoted by **P** in Fig. 2), whose difference represents the real pressure drop across the filter.

The filter was loaded through a synthetic soot generator (Aerosol Generator GFG-1000-PALAS) at a gas flow rate of 46 l/min (argon 6 l/min + air). The soot mass flow rate was 5 mg/h. Synthetic soot was employed in order to achieve reproducible data, since real diesel soot features would be indeed too much dependent on the ever-changing engine conditions. As a matter of fact, the presence of adsorbed hydrocarbons in real soot particles introduces a difficult predictability of the aggregation phenomena due to an enhanced sticking factor, while in the regeneration phase (not treated in this work) it determines the actual reactivity of the deposited cake layer [16]. Two loading times were investigated, namely 7.8 h and 24 h. This approach was tailored to the investigation of soot deposition profiles at different filtration times.

The experimental procedure to measure the cake thickness inside the channels of the filter was based on images from field emission scanning electron microscopy (FESEM-Leo 50/50 VP with Gemini column): at the end of the loading process, the filter was peripherally cut at different axial positions, and then gently broken into segments. As a result, the structure of the cake layer in the channels not involved by the cutting procedure was perfectly preserved. The cake thickness was evaluated in the channels of each segment, along one diameter of the filter (channels 1–7 as depicted in Fig. 3), except for the most peripheral ones that are sensitive to the cutting operation and therefore not representative.

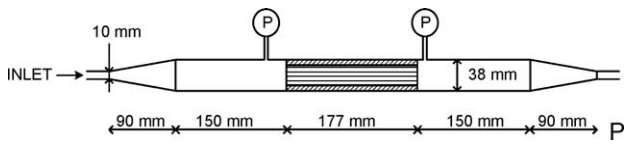

Fig. 2. Sketch of the second filter housing.

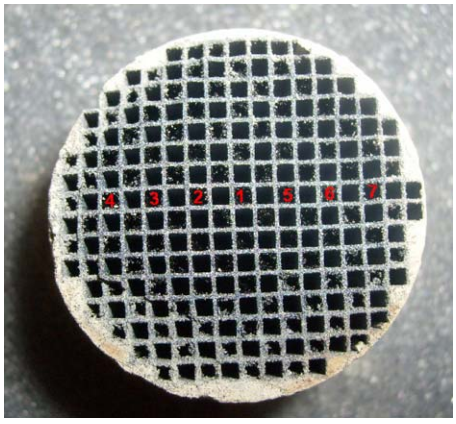

Fig. 3. Segment from the lab-scale filter, loaded with the synthetic soot from the aerosol generator, with the channels labelling.

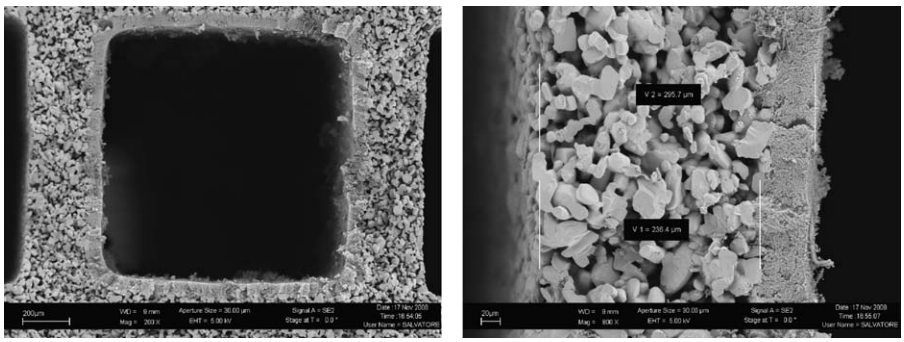

Fig. 4. Thickness of the soot layer (SEM figures): the whole channel (left – 200×) and a detail of the cake thickness measurement in one side of the channel (right – 800×).

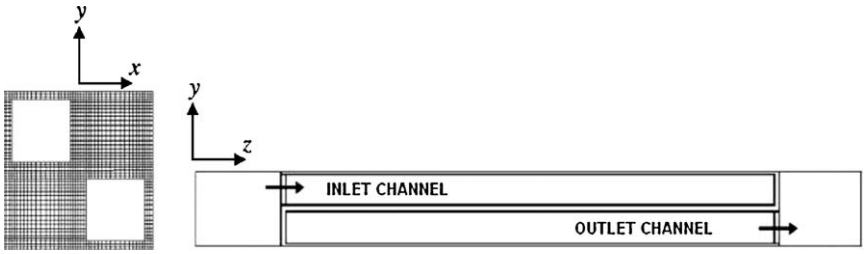

Fig. 5. Sketch of the grid used to simulate a periodic structure of channels in a DPF.

The soot layer thickness was measured in all sides of the channel, and then averaged (Fig. 4).

The filtration efficiency of the DPF was evaluated by measuring the soot particle size distribution produced by the aerosol generator in the above mentioned conditions and the one exiting the filter. The particle distributions were measured with a Scanning Mobility Particle Sizer (SMPS by TSI Inc. with 3080 electrostatic classifiers and Dekati volumetric diluter operating at room temperature with a dilution ratio of 10), with sampling frequency of 5 min.

The mathematical description of this system was carried out under different simplification hypotheses and at two different scales: the first one consisted of considering all the filter channels at the same operating conditions, namely with a inlet mass flow rate calculated as the total flow over the number of the open channels. Following this approach, the three-dimensional geometry adopted to simulate the "channel scale" consisted of four modelled channels, two of them allowing the gas to enter the filter, while the other two being plugged (see Fig. 5); at the end of the filter, plugs are reversed. Before the inlet of the filter, there is an upstream region where a flat velocity profile is set. As far as the boundary conditions of the domain are concerned, the lateral faces were set as periodic. This allowed modelling the behaviour of wall flow monoliths, characterized by a periodic structure of hundreds of cells per square inch, in the hypothesis that an even flow rate entered in each DPF channel. Details on these calculations and on their implementation in the computational fluid dynamics (CFD) code Fluent through user-defined-subroutines can be found in our previous works [14,15].

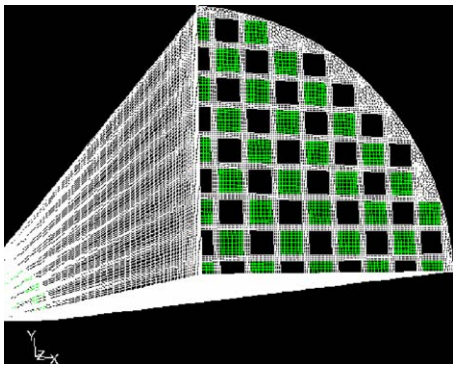

Fig. 6. Sketch of the grid used to simulate the full-scale DPF.

The other approach was to compute the actual flow rate into the filter channels, and therefore to take into account the maldistribution of the gas flow at the filter inlet. To this end, the so called "full-scale" grid included the complete geometrical representation of the filter housing, from which the DPF grid is shown in Fig. 6. The grid was created on the basis of the geometrical details of both housings and, for symmetrical reasons, only one fourth of the geometries were reproduced. The aim of adopting the full-scale grid was to solve explicitly the flow field inside the filter housing, and therefore to be able to predict the proper gas flow rate entering each channel of the filter. The relationship between the models and the experimental data are detailed in the next section.

3. Results and discussion

The outcome of the experimental campaign, focused on the cake thickness evaluation, is here reported and discussed. Fig. 7 shows the deposition profiles of soot inside the channels of a filter canistered as in Fig. 1. The experimental points in Fig. 7-left represent the cake thicknesses along the axial coordinate for different channels. From these data it arises that the filter was not uniformly loaded with respect to the radial coordinate: lateral channels were less involved in the filtration process than the ones located in the central part of the filter. This behaviour can be seen clearly in Fig. 7-right, where the soot layer thickness is depicted for channels from 1 to 7, along the filter diameter, at one specific axial coordinate. Such a maldistribution of the gas flow into the filter channels was due to the persistence of a gas jet velocity profile, generated in correspondence to the 6 mm pipe outflow, and not dissipated in the cone. This phenomenon occurs also in a real full-scale DPF, if not coupled to an upstream DOC, since the adduction pipe is far smaller than the monolith's diameter and an uneven distribution of the gas into the channels occurs. If one focuses on

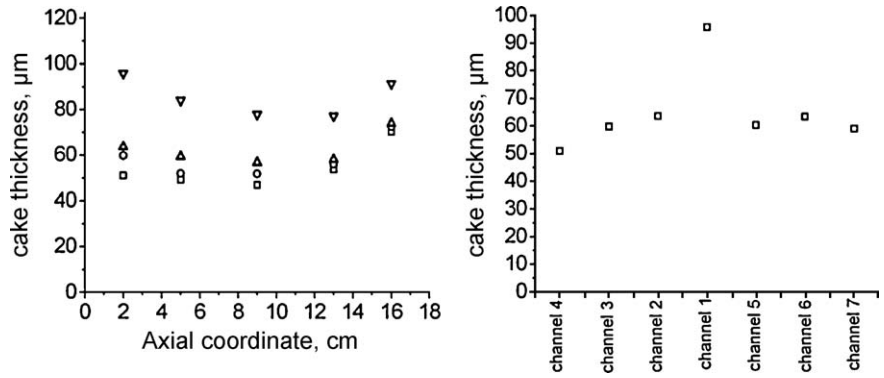

Fig. 7. Experimental thickness of the soot layer along the filter, housed as in Fig. 1, for a loading time of 24 h. Left: different axial positions (▽-channel 1, Δ-channel 2, ○-channel 3, □-channel 4); right: channel locations (face at $z = 2$ cm) [12].

the mean thickness of the soot layer with respect to the axial coordinate (Fig. 7-left), it appears that the cake has a minimum thickness at around half of the total filter length, while the edges are more heavily loaded since there the velocity was higher. This is in agreement with our past simulations of soot filtration in DPFs [14,15].

The second configuration of the filter housing, depicted in Fig. 2, reduced considerably the effects of maldistribution at the filter inlet, as can be seen by the measurements of cake thickness in Fig. 8 (obtained with the same procedure as described for Figs. 3 and 4). In the cake thickness representation of Fig. 8, channels 4 and 7 are excluded since they are the most peripheral ones and were slightly involved in the cutting operation. A certain dispersion of the cake thickness in the channels is observed at 5 cm and 9 cm from the inlet, but no clear accumulation in one or some of the channels emerges as in Fig. 7 in correspondence of channel 1. Apart from the differences in cake accumulation, the same trend along the axial coordinate is found in the two housing systems, leading to a greater concentration at the beginning and the end of the filter channel. As described in our previous work [13], which resorted to the channel scale grid, this feature was not due to inertial effects, that might cause a deviation of the particle trajectories from the streamlines of the fluid and their entrainment at the end of the filter. Indeed, soot particles produced by the aerosol generator are commonly below 200 nm, for which inertial effects are negligible. As a matter of fact, such an accumulation is induced by the peculiar profile of the through-wall velocity of both gas and particles, that has a minimum at approximately half of the total channel length. At the beginning of the filtration process, the soot deposition rate has a profile very similar to the one of the gas through-wall velocity, since particles are carried by the gas showing negligible inertial effects. After soot has started to deposit, the increased viscous resistance modifies the gas through-wall velocity to a flatter profile [13] and this leads to the soot layers observed experimentally.

The cake thickness evolution was investigated also at lower filtration times: Fig. 9 shows the profile of soot accumulation inside the channels of the filter, housed as in Fig. 2 to allow a better distribution of the flow inside the channels, at the end of a filtration process lasting 7.8 h. Some differences appear between Fig. 9 and Fig. 8, the latter corresponding to a loading process in the same operating conditions, but approximately three times longer. It appears clearly from Fig. 9 that the minimum of soot thickness along the axial coordinate was closer to the inlet rather than in Fig. 8: this was probably due to the fact that cake formation started at the end of the filter [14,15], since the filter experiences just there the highest soot mass flow (and deposition) rates. However, as long as filtration proceeds, the deposited soot caused a higher and higher local pressure drop, and therefore also the middle and the initial part of the filter became fully involved in the processes of cake formation and thickening. Further tests at shorter loading times are ongoing, in order to construct a detailed curve of cake evolution along the axial coordinate with respect to the filtration time. Another feature of Fig. 9 is that the soot thickness was almost half of the one seen in Fig. 8, even if the loading time was three times smaller. This suggests that the soot packing density could have varied along the process according to the increased pressure drop, as observed also in the literature [10].

During soot loading, the pressure drop across the filter was recorded. In the first housing, this was done by measuring the

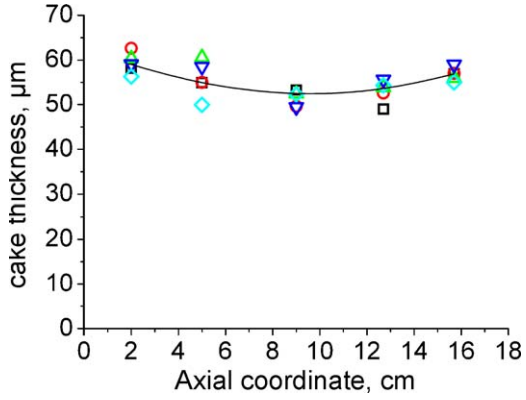

Fig. 8. Experimental thickness of the soot layer along the filter, housed as in Fig. 2, for a loading time of 24 h (Δ-channel 1, ○-channel 2, □-channel 3, ▽-channel 5, ◇-channel 6, solid line-mean value).

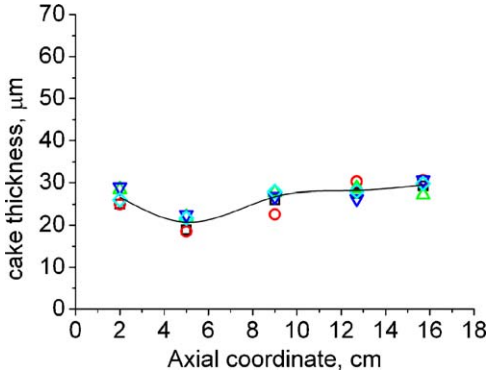

Fig. 9. Experimental thickness of the soot layer along the filter, housed as in Fig. 2, for a loading time of 7.8 h (Δ-channel 1, ○-channel 2, □-channel 3, ▽-channel 5, ◇-channel 6, solid line-mean value).

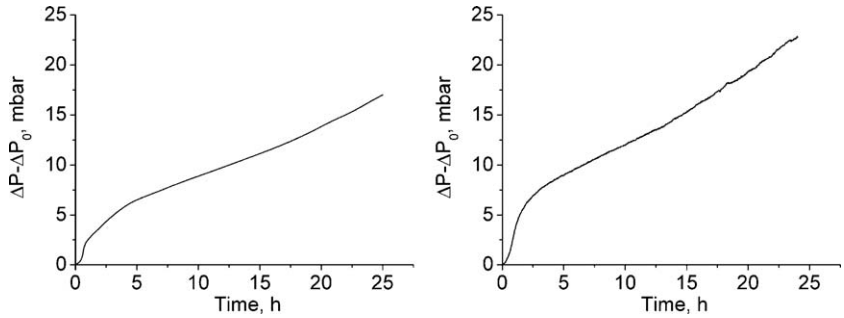

Fig. 10. Pressure drop increase measured across filters housed as in Fig. 1 (left) and 2 (right), for a loading time of 24 h.

relative pressure before the filter inlet, while in the second case it was obtained as the difference between the pressure before and after the filter itself. The two pressure drop profiles are compared in Fig. 10 for the 24 h lasting test. The increase of pressure drop with respect to the initial one was depicted. The bare filter pressure drop measured in the first housing (Fig. 10-left) was 21.5 mbar, which was considerably higher than the 3 mbar recorded in the second one (Fig. 10-right). This is due to the fact that the sampling point was before the conic junction in the former case, thus accounting for both the filter pressure drop and the loss caused by gas expansion effects. Fig. 10 showed in both plots a loss of linearity in the last part of the curve, because of a reduced open area available for the gas, which increased the gas velocity (and the friction) inside the channels. The maldistribution at the filter inlet and the unevenness of soot deposition in the filter channels was found to slightly influence the slope of the pressure drop curve. However, due to the limited number of channels involved by such maldistribution, this effect was not severe. Soot deposition profiles have also another important implication: during regeneration, depending on the ignition temperature and on the oxygen concentration, the soot cake burns with different rates according to its deposition profile inside the filter. Since the time scale of the soot ignition is very small, when soot ignites then local temperature gradients become immediately quite high [8]. If in some regions an excessive amount of deposited soot occurs due to the maldistribution of the inlet flow, the high heat released during combustion could cause cracks or melting of the porous support [12].

As far as the filtration efficiency of the DPF is concerned, Fig. 11 depicts the measured particle size distribution at the inlet and the outlet of the filter, housed as in Fig. 2. The loading process lasted 7.8 h, and the sampling frequency was 5 min. Fig. 11 reports the measured particle size distribution times the dilution ratio (i.e. the real particle concentration in the gaseous flow), and it includes the first 85 min of the overall filtration process, since at that point almost all particles were filtered. The initial filtration efficiency was greater than 85% on a mass (or volumetric) basis. Brownian motions were the most important collection mechanism, since particles were quite small [4,11] (below 200 nm) and the through-wall velocity was in the order of cm/s, as discussed in [12]. The mean particle diameter, based on the total number of particles, was measured thorough the SMPS: it was found to be around 65 nm at the beginning of the filtration process, while after 85 min it decreased to 52 nm, highlighting the improved ability of the filter to collect smaller particles, due to the intrinsic filtration process operated by the cake layer.

In order to correlate the stages of the loading process and the filtration efficiency, Fig. 12 shows the two quantities in the time-frame of the whole experiment. The steps of soot filtration are here clearly visible: first, soot accumulated in the pores of the filter wall, causing a progressive modification of the filter porosity, permeability and collection efficiency. After approximately 1 h the filter reached a filtration efficiency of 99.8%, the process being at an intermediate point of the cake building phase. Subsequently, the soot layer completely occluded filter pores (cake filtration step), thus evolving towards a steady increase of the pressure drop, indicating the progressive thickening of the cake with time [5]. As a matter of fact, our ongoing experimental campaign is focused on the experimental investigation of soot deposition profiles at times corresponding to the cake building phase, to observe their influence on the integral filtration efficiency.

It should be pointed out that the pressure drop curves in Fig. 12 and Fig. 10-right slightly differ in terms of slope, although the two experiments were carried out under the same operating condi-

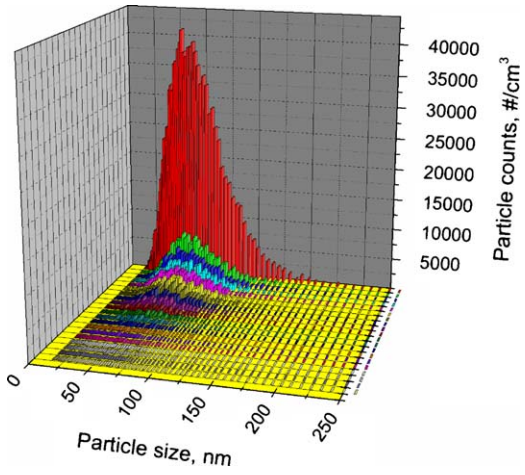

Fig. 11. Soot particle size distribution determined by Scanning Mobility Particle Sizer at the inlet (red) and the outlet (other colours) of the filter, housed as in Fig. 2, for the first 85 min of a total loading time of 7.8 h and a sampling frequency of 5 min. (For interpretation of the references to color in this figure legend, the reader is referred to the web version of the article.)

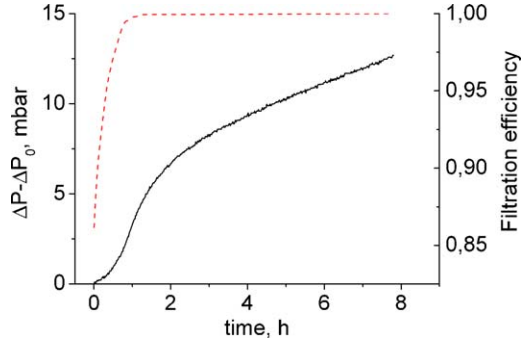

Fig. 12. Pressure drop (black solid line-left axis) and filtration efficiency on a mass basis (red dashed line-right axis), measured on a tested filter housed as in Fig. 2, for a loading time of 7.8 h. (For interpretation of the references to color in this figure legend, the reader is referred to the web version of the article.)

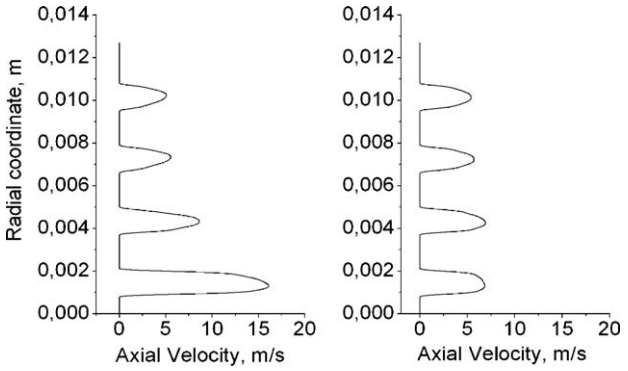

Fig. 13. Computed axial component of the inlet velocity into the bare filter, housed as in Fig. 1 (left) and Fig. 2 (right).

tions. This is probably due to the fact that such processes suffer from a certain variability ascribed to the canistering operation and the flow field in front of the filter.

A detailed prediction of the soot deposition profiles inside the channels of the filter through a mathematical model is useful to tailor the trap design, both to accumulate soot through patterns allowing low pressure drops, and to drive a "safe" regeneration with no major thermal cracks produced by hot spots (also in the perspective of catalytically coated filters, currently under investigation). As explained in the literature, the effect of the inlet maldistribution has to be accounted to perform a correct modelling of the soot loading and regeneration steps; this was operated through the efficient coupling of the different scales of a DPF, namely the full filter scale, the channel scale and the porous wall scale [12,13].

To this end, two computational grids were adopted to simulate this system with the CFD code: the channel-scale grid and the filter-scale grid. The channel scale grid (in our code including also the porous wall discretization) is based on the hypothesis that an even flow rate enters in each DPF channel. Hence, the model simulates the flow field of the gas and soot particles in a single channel, and it predicts the cake profile on the filter porous walls as well as the associated evolution with time of the pressure drop [14,15]. However, as demonstrated by the experimental data belonging to the DPF housing in Fig. 1, the assumption of considering the DPF channels as a periodic structure can be erroneous.

The full-scale grid was aimed at solving the flow field inside the filter housing, and therefore this grid gives the actual inlet flow rate into each channel, depending on its radial position. As a preliminary result, Fig. 13 shows the computed inlet velocities into the DPF channels along a filter radius, at the beginning of the filtration process (bare filter). It is clearly visible that a strong maldistribution of the flow was predicted in the case of first test-rig (Fig. 13-left), since the gas inlet from the 6 mm pipe was very close to the DPF frontal surface. Moreover, the gas strongly decelerated when approaching to the DPF inlet, thus being forced to re-circulate back, with the consequence that the inflow in the channels was not perpendicular to the inlet DPF surface. The ongoing investigation is focussed on optimizing computational costs arising from the coupling of the two scales models, during the soot loading phase.

4. Conclusions

Features of cake deposition profiles inside the channels of a DPF are here investigated. Our experimental procedure allowed collecting soot under real loading conditions, and gaining reliable information about the axial deposition profiles inside the different channels of a DPF. Experimental FESEM observations reveal that the soot layer thickness is not constant along the axial coordinate, being minimum at around half of the channel length, as supported and explained by our CFD simulations. In addition, depending on the distribution of the gaseous flow at inlet of the filter, the behaviour of soot deposition is greatly affected by the channel position with respect to the radial coordinate. It emerges that, according to the filter housing and the inlet flow pipes, a strong gas maldistribution could occur at inlet of the filter itself, thus making some channels far more loaded of soot rather than others.

From the analysis of deposition profiles at a shorter loading time, still in the same operating conditions, one can observe that the inlet part of the filter is slightly less involved in cake thickening rather than the end of the filter. Another important outcome of this campaign is the correlation between the pressure drop, and therefore of the soot layer growing, with the filtration efficiency, which highlights the filtering effect of the soot layer.

These observations have some important implications in the regeneration step, since soot combustion has to be carried out uniformly inside the filter, and in particular without unpredicted heat releases in some points, due to an excessive soot accumulation.

A multi-scale model for the description of soot filtration through DPFs is finally discussed: beside the channel scale model, which was already presented in past papers, a full-scale model is under development, in order to reproduce the features encountered in the experimental SEM observations.

References

[1] H.G. Neumann, Chemosphere 42 (2002) 473–479.
[2] S.H. Ye, W. Zhou, J. Song, B.C. Peng, D. Yuan, Y.M. Lu, P.P. Qi, Atmospheric Environment 34 (1999) 419–429.
[3] C.A. Pope III, R.T. Burnett, G.D. Thurston, M.J. Thun, E.E. Calle, D. Krewski, J.J. Godleski, Circulation 109 (2004) 71–77.
[4] E. Ohara, Y. Mizuno, Y. Miyairi, T. Mizutani, K. Yuuki, Y. Naguchi, T. Hiramatsu, M. Makino, A. Takahashi, H. Sakai, M. Tanaka, A. Martin, S. Fujii, P. Busch, T. Toyoshima, T. Ito, I. Lappas, C.D. Vogt, SAE 2007-01-0921, 2007.
[5] A. Suresh, A. Khan, J.H. Johnson, SAE 2000-01-0476, 2000.
[6] E. Cauda, D. Fino, G. Saracco, V. Specchia, Chemical Engineering Science 62 (2007) 5182–5185.
[7] T. Deuschle, U. Janoske, M. Piesche, Chemical Engineering Journal 135 (2008) 49–55.
[8] G.C. Koltsakis, A.M. Stametelos, Industrial & Engineering Chemical Research 36 (1997) 4155–4165.
[9] C.S. Yoon, S.H. Song, K.M. Chun, 2007-01-0311, 2007.
[10] G.C. Koltsakis, A. Konstantinou, O.A. Haralampous, Z.C. Samaras, 2006-01-0261, 2006.
[11] E. Wirojsakunchai, E. Schroeder, C. Kolodziej, D.E. Foster, N. Schmidt, T. Root, T. Kawai, T. Suga, T. Nevius, T. Kusaka, SAE 2007-01-0320, 2007.
[12] A.G. Konstandopoulos, M. Kostoglou, P. Housiada, N. Vlachos, D. Zarvalis, SAE 2003-01-0839, 2003.
[13] G.C. Koltsakis, O.A. Haralampous, N.K. Margaritis, Z.C. Samaras, C.-D- Vogt, E. Ohara, Y. Watanabe, T. Mizutani, SAE 2005-01-0953, 2005.
[14] S. Bensaid, D.L. Marchisio, D. Fino, G. Saracco, V. Specchia, Chemical Engineering Journal, doi:10.1016/j.cej.2009.03.043, in press.
[15] S. Bensaid, D.L. Marchisio, D. Fino, G. Saracco, V. Specchia, in: Proceedings of the 10th World Filtration Congress, Leipzig, Germany, April 3, (2008), pp. 328–332.
[16] D. Fino, N. Russo, F. Millo, D.S. Vezza, F. Ferrero, A. Chianale, New tool for experimental analysis of diesel particulate filter loading, in: CAPoC8 Proceedings, 2009, P91.